Space-time clutter rejection using the *APES* method

Jacques Raout [#1], Agnès Santori [#2]

[#] *MorphoAnalysis in Signal processing Lab., Research Center of the French Air Force*
13 661 Salon de Provence, France
[1] jacques.raout@inet.air.defense.gouv.fr
[2] agnes.santori@inet.air.defense.gouv.fr

***Abstract*— A new method to reject ground clutter using the Amplitude and Phase EStimation (*APES*) method is proposed in this paper. The theoretical approach is followed by the application of this method on the rejection of such an interference in the frame of a bistatic passive radar using Digital Video Broadcasting -Terrestrial ($DVB-T$) transmitters.**

I. Introduction

Radars using illuminators of opportunity are inherently passive bistatic radars. The passivity of bistatic radars offers definitive advantages namely low cost, low weight and enhanced radar cross-section for certain geometries. Moreover, stealth operations are possible since the receiver is totally passive.

Furthermore, noise-like signals allow unambiguous range and Doppler estimation and an independent control of Doppler and range measurements. Their ambiguity function presents no side lobes (just noise floor), and high rate compression is possible. In addition, they behave very favorably against Electronic CounterMeasures (Anti Radar Missile (*ARM*) and jamming). They also exhibit better performance in Low Probability of Interception (*LPI*) and Exploiting (*LPE*). In the ElectroMagnetic Compatibility (*EMC*) domain, better interference immunity and the possibility of using many radars simultaneously within the same area are expected.

Radars using illuminators of opportunity have already been studied. Signals provided by FM radio broadcast [1], satellites [2],digital video broadcast ($DVB-T$) [3], and Global System for Mobile communications (*GSM*) base stations [4]have been considered. Arguments for the selection of the transmitter type include spatial and time coverage, power, central-frequency and bandwidth of the emitted signal, and shape of the ambiguity function. The bandwidth dictates the achievable range-resolution and the shape of the ambiguity function is decisive in determining the detection performance of the radar. In particular, signals from digital modulation (*GSM*, $DVB-T$) have much less range and Doppler ambiguities than other modulations [5], which makes them more suitable for passive radar. In this paper, we will consider DVB-T transmitters as illuminators of opportunity. They have a ubiquitous spatial coverage, are permanent in time and have a thumbtack like ambiguity function due to the noise-like behavior of the $OFDM$ modulation used.

Space-Time Adaptive Processing (*STAP*) is typically used to filter out (clutter-) interferences in $GMTI$ radars in order to detect slow-moving targets. *STAP* offers a benefit over separate spatial and temporal processing when there is a coupling between the clutter signal direction of arrival (*DOA*) and its Doppler frequency. *STAP* consists in performing a joint spatio-temporal optimum filtering of the signal in order to reject interference (clutter) contributions [6], [7].

Classical *STAP* methods such as the Principal Components (*PC*) method [7], [8], reduced rank methods such as the Joint Domain Localized (*JDL*) method [8], [9] or the hybridization of the *JDL* method with the Direct Data Domain (D^3) method [10]–[12] involve to estimate the covariance matrix of the interferences. Their performance can suffer from the presence of discrete sources of interference, the lack of homogeneous range cells for the estimation of the covariance matrix and the non-Gaussianity of the environment.

We propose in this paper not to use the covariance matrix but to iteratively reject components of the clutter using the *APES* method. This method can not be considered as adaptative but need an a priori knowledge of the clutter power spectral density locus.

The paper is organized as follows. Section 2 depicts the reference signal model, namely, $DVB-T$ signal characteristics and the received signal model, made of the signal of interest (the target), clutter and noise.

Section 3 is dedicated to the adaptation to noise-like signals of the *APES* method.

Finally, section 4 describes results of the bistatic passive detection of a simulated target added to real clutter created by a $DVB-T$ transmitter of opportunity.

<u>Notations</u>: *, ^{T}, †, $\hat{}$ represent respectively the conjugate, transpose, Hermitian transpose and estimate of a vector/matrix. The element corresponding to the column c and line l of a matrix $\mathbf{M}$ will be represented by M_{lc}, its line index l by $\mathbf{M}_l$. The C first values of a vector $\mathbf{v}$ will be represented by $\mathbf{v}_C$, its l^{th} element by v_l, the portion of this vector between elements i and j by $\mathbf{v}_{i:j}$.

The identity matrix with dimension N will be written $\mathbf{I}_N$, $\mathbf{c}_C$ is the column vector with C unit elements, $\mathbf{0}_N$ the column vector with C null elements, $\mathbf{l}_L$ is the row vector with L unit elements. $\mathbf{J}_N$ is the exchange or reflection matrix (i.e., a matrix of dimension N that has ones along its anti-diagonal, and zeros everywhere else).

The Kronecker product is represented by $\otimes$, the Hadamard product by $\circ$. If we consider a $N \times M$ matrix $\mathbf{A}$, the vec-function of $\mathbf{A}$ is written $vec(\mathbf{A})$ and is obtained by stacking the columns to get a $NM \times 1$ vector.

II. Signal model

Let us consider a sampled space-time signal $\mathbf{Y}$, made of clutter, potential target and noise, received by a sparse array antenna made of N_s elements, during a coherent integration time T_{ci} corresponding to N_d samples, so that $T_{ci} = \frac{N_d}{f_s}$ with f_s the sampling frequency. The inter-element spacing between the $i+1^{th}$ antenna element and the previous one is represented by $d_{i+1,i}$ and the carrier wavelength by λ.

The various components of the received signal are defined by their amplitude, delay compared to the direct path, reduced Doppler frequency and associated steering vector in the temporal domain and direction of arrival linked to the steering vector in the spatial domain.

The general expression of a temporal steering vector in the direction of the reduced Doppler frequency $\nu_d = \frac{f_d}{f_s}$ with f_d the Doppler frequency is given by:

$$\begin{aligned} \mathbf{s}_d(\nu_d) &= \left[1, e^{j2\pi\nu_d}, \ldots, e^{j2\pi\nu_d(N_d-1)}\right]^T \\ &= \left[1, z_d(\nu_d), \ldots, z_d^{N_d-1}(\nu_d)\right]^T \end{aligned} \quad (1)$$

where $z_d(\nu_d)$ stands for the temporal phase shift from one sample to another due to the motion of the considered component.

In the case of a sparse array (specifically used for real measurements presented in this paper), the spatial steering vector in the direction of arrival θ is:

$$\begin{aligned} \mathbf{s}_s(\theta) &= \left[1, e^{j2\pi\frac{\sin(\theta)}{\lambda}d_{2,1}}, \ldots, e^{j2\pi\frac{\sin(\theta)}{\lambda}\sum_{i=1}^{N_s-1}d_{i+1,i}}\right]^T \\ &= \left[z_{s_{1,0}}(\theta), z_{s_{2,1}}(\theta), \ldots, \prod_{i=1}^{N_s-1} z_{s_{i+1,i}}(\theta)\right]^T \end{aligned} \quad (2)$$

where $z_{s_{i+1,i}}(\theta)$ stands for the spatial phase shift from the $i+1^{th}$ antenna element to the previous element. By convention, $z_{s_{1,0}}(\theta)$ is chosen equal to 1.

The space-time steering vector is deduced from both spatial and temporal steering vector:

$$\mathbf{s}(\theta, \nu_d) = \mathbf{s}_d(\nu_d) \otimes \mathbf{s}_s(\theta) \quad (3)$$

The clutter signal $\mathbf{Y}_c$ is assumed to be made of the total contribution of N_r interfering range cells, creating multipaths. Each range cell is made of $N_{r;p}$ contributing clutter patches with complex amplitude $\alpha_{r;p}$, delay $\tau_r = \frac{r}{f_s}$, spatial steering vector $\mathbf{s}_s(\theta_r)$ linked to the angle θ_r:

$$\begin{aligned} \mathbf{Y}_c &= \sum_{r=1}^{N_r}\sum_{p=1}^{N_{r;p}} \mathbf{Y}_{c_{r;p}} \\ &= \sum_{r=1}^{N_r}\sum_{p=1}^{N_{r;p}} \alpha_{r;p}\mathbf{s}_s(\theta_r)\left(\mathbf{x}(-\tau_r) \circ \mathbf{s}_d(\nu_{d_{r;p}})\right)^T \end{aligned} \quad (4)$$

with the general expression for the processed part of the reference signal:

$$\mathbf{x}(-\tau_r) = \left[x\left(\frac{1-r}{f_s}\right), x\left(\frac{2-r}{f_s}\right), \cdots, x\left(\frac{N_d-r}{f_s}\right)\right]^T \quad (5)$$

The signal is also supposed to be made of the signal, $\mathbf{Y}_t$, from a target with complex amplitude α and located at angle θ, reduced Doppler frequency ν_d and bistatic delay τ.

$$\begin{aligned} \mathbf{Y}_t &= \alpha\mathbf{s}_s(\theta)\left(\mathbf{x}(-\tau) \circ \mathbf{s}_d(\nu_d)\right)^T \\ &= \alpha\left(\mathbf{c}_{N_s} \otimes \mathbf{x}^T(-\tau)\right) \circ \left(\mathbf{s}_s(\theta) \otimes \mathbf{s}_d^T(\nu_d)\right) \\ &= \alpha\mathbf{X}(-\tau) \circ \left(\mathbf{s}_s(\theta) \otimes \mathbf{s}_d^T(\nu_d)\right) \end{aligned} \quad (6)$$

Noise is represented by $\mathbf{N}$, an ergodic, stationary and zero mean random process.

One can see in this model that clutter is considered as a finite sum of discrete contributors. Under this assumption, we propose to use a spectral estimation method, namely the *APES* method, to determine the amplitude, Doppler and angle of the main contributors and to subtract their contribution from the received signal, one after the other.

III. Generalization of the *APES* method to noise-like signals

In the case of a bistatic radar exploiting a noise-like signal, a way to adapt the *APES* method [13]–[15] is to work on the mixing product defined for each range r associated to the delay τ by:

$$\mathbf{Y}_m(\tau) = \mathbf{Y}(\tau) \circ \left(\mathbf{c}_{N_s} \otimes \mathbf{x}^\dagger\right) \quad (7)$$

In an analog way, we will no longer consider the reference signal or the noise signal but their mixed version, $\mathbf{X}_m$ and $\mathbf{N}_m(\tau)$.

Since the contributors induce a Doppler frequency that is much smaller than the sampling frequency, the signal can be low-pass filtered and subsampled as suggested in [16]. The subsampling factor will be noted S. Note that this subsampling does not affect the range-resolution of the radar.

The reduced Doppler frequency after this processing will be noted $\tilde{\nu}_d = \nu_d S$.

Low-pass filtering and subsampling play an important role in the adaptation of the *APES* method to noise-like signal. Both the demodulation, represented by the Hadamard product of a delayed version, regarding the considered range cell, of the received signal by the reference one (see equation (7)) and low-pass filtering plus subsampling allow the noise-like signal to get closer to a Doppler shifted pulse with a low level of amplitude fluctuations.

This processing is associated to the subsampling and low-pass filtering matrix:

$$
\begin{aligned}
\mathbf{S}(\nu_d) &= e^{-j\pi(S-1)\nu_d}\frac{\sin(\pi\nu_d)}{\sin(\pi\tilde{\nu}_d)}\begin{bmatrix} \mathbf{c}_S & \mathbf{0}_S & \cdots & \cdots & \mathbf{0}_S \\ \mathbf{0}_S & \mathbf{c}_S & \mathbf{0}_S & \cdots & \mathbf{0}_S \\ \vdots & \ddots & \ddots & \ddots & \vdots \\ \vdots & \ddots & \ddots & \ddots & \vdots \\ \mathbf{0}_S & \cdots & \cdots & \mathbf{0}_S & \mathbf{c}_S \end{bmatrix} \\
&= \iota(\nu_d)\mathbf{I}_{\frac{N_d}{S}} \otimes \mathbf{c}_S
\end{aligned} \tag{8}
$$

The correction by the coefficient $\iota(\nu_d) = \frac{1}{\sum_{S-1}^{k=0} e^{2j\pi k\nu_d}}$ is necessary to compensate the effect of subsampling on the temporal steering vector. It yealds:

$$
\mathbf{S}^T(\nu_d)\mathbf{s}_d(\nu_d) = \tilde{\mathbf{s}}_d(\tilde{\nu}_d) \tag{9}
$$

The mixed signal defined in equation (7), for example, will now be replaced by:

$$
\begin{aligned}
\tilde{\mathbf{Y}}(\tau,\nu_d) &= \mathbf{Y}_m(\tau)\mathbf{S}(\nu_d) \\
&= \iota(\nu_d)\mathbf{Y}_m(\tau)\mathbf{S} \\
&= \iota(\nu_d)\tilde{\mathbf{Y}}(\tau)
\end{aligned} \tag{10}
$$

One can see on the previous equation that it is not necessary to take into account a different mixed, low-pass filtered and subsampled signal $\tilde{\mathbf{Y}}(\tau,\nu_d)$ for each temporal direction but to work with $\tilde{\mathbf{Y}}(\tau)$ and to apply the correction.
$\tilde{\mathbf{X}}$ and $\tilde{\mathbf{N}}(\tau)$ would be defined in the same way from $\mathbf{X}_m$ and $\mathbf{N}_m(\tau)$ respectively.
The number of processed blocs, made of subsampled and low-pass filtered data, $\frac{N_d}{S}$ will be noted $\tilde{N}_d$.
Considering the mixed, low-pass filtered and subsampled signals, the purpose, for each step of the iterative rejection process, is to estimate the maximal amplitude $\hat{\alpha}_{r;p}$ corresponding to the main contributor so that:

$$
\hat{\tilde{\mathbf{Y}}}_{c_{r;p}}(\tau) = \hat{\alpha}_{r;p}\tilde{\mathbf{X}} \circ \left(\mathbf{s}_s(\theta_p)\tilde{\mathbf{s}}_d^T(\tilde{\nu}_{d_{r;p}})\right) \tag{11}
$$

To facilitate readers understanding, the reference to the range cell (τ) and the spatio-temporal direction $(\theta_p, \tilde{\nu}_{d_{r;p}})$ scanned during the processing will be suppressed.
Applying the *APES* method implies to work with $\tilde{\mathbf{y}}_{i;l}$:

$$
\tilde{\mathbf{y}}_{i;l} = vec\left(\tilde{\mathbf{Y}}_{i:i+M_s-1,l:l+\tilde{M}_d-1}\right) \tag{12}
$$

and

$$
\tilde{\Upsilon} \triangleq \left[\tilde{\mathbf{y}}_{1;1}, \cdots, \tilde{\mathbf{y}}_{L_s;1}, \tilde{\mathbf{y}}_{1;2}, \cdots, \tilde{\mathbf{y}}_{L_s;\tilde{L}_d}\right] \tag{13}
$$

The values of M_s, $\tilde{M}_d$, L_s and $\tilde{L}_d$ are chosen so that $\tilde{\mathbf{Y}}$ is a square matrix ($L_s\tilde{L}_d = M_s\tilde{M}_d$). In addition, the number of antenna elements of the sparse array being small ($N_s = 4$), M_s is chosen equal to N_s leading to $L_s = 1$ ($L_s = N_s - M_s + 1$). Once the integration time and the subsampling factor are chosen and using $\tilde{L}_d = \tilde{N}_d - \tilde{M}_d + 1$, we obtain:

$$
\tilde{M}_d = \frac{\tilde{N}_d - N_s + 1}{N_s} \tag{14}
$$

Furthermore, we will note $\tilde{\mathbf{x}}$ the first column of the matrix $\tilde{\mathbf{X}}^T$. This leads us to the optimization problem:

$$
\min_{\mathbf{h},\hat{\alpha}} \|\mathbf{h}^\dagger\tilde{\Upsilon} - \hat{\alpha}\tilde{\mathbf{x}}_{\tilde{L}_{sd}} \circ \tilde{\mathbf{s}}_{\tilde{L}_{sd}}\|^2 \tag{15}
$$

with the constraint

$$
\mathbf{h}^\dagger(\tilde{\mathbf{x}}_{\tilde{M}_{sd}} \circ \tilde{\mathbf{s}}_{\tilde{M}_{sd}}) = 1 \tag{16}
$$

$\mathbf{h} \in \mathbb{C}^{M_s\tilde{M}_d}$ is the vector containing the coefficients of the filter at the frequency $(\theta, \tilde{\nu}_d)$ for the considered range cell.

Proposition 1 (Noise APES (NAPES filter)): The solution of the optimization problem (equation (15)) under the constraint (equation(16)) is:

$$
\hat{\alpha} = \mathbf{h}^\dagger\tilde{\mathbf{g}} \tag{17}
$$

and

$$
\mathbf{h} = \frac{\hat{\tilde{\mathbf{Q}}}^{-1}\tilde{\mathbf{x}}^{sd}_{\tilde{M}_{sd}}}{\left(\tilde{\mathbf{x}}^{sd}_{\tilde{M}_{sd}}\right)^\dagger\hat{\tilde{\mathbf{Q}}}^{-1}\tilde{\mathbf{x}}^{sd}_{\tilde{M}_{sd}}} \tag{18}
$$

where

$$
\tilde{\mathbf{g}} = \frac{1}{\|\tilde{\mathbf{x}}_{\tilde{L}_{sd}}\|^2}\tilde{\Upsilon}\left(\tilde{\mathbf{x}}^{sd}_{\tilde{L}_{sd}}\right)^* \tag{19}
$$

$$
\hat{\tilde{\mathbf{Q}}} = \frac{1}{\|\tilde{\mathbf{x}}_{\tilde{L}_{sd}}\|^2}\tilde{\Upsilon}\tilde{\Upsilon}^\dagger - \tilde{\mathbf{g}}\tilde{\mathbf{g}}^\dagger \tag{20}
$$

$\tilde{\mathbf{x}}^{sd}_{\tilde{M}_{sd}} = \tilde{\mathbf{x}}_{\tilde{M}_{sd}} \circ \tilde{\mathbf{s}}_{\tilde{M}_{sd}}$ is obtained from the reference signal, mixed, lowpass filtered, subsampled and steered in the desired spatio-temporal direction and $\|\tilde{\mathbf{x}}_{\tilde{L}_{sd}}\|^2 = L_s\sum_{l=1}^{\tilde{L}_d}|\tilde{x}_l|^2$.
Range cells index r are processed one after the other. Once the Doppler, angle and amplitude of the main contributor to clutter in this range cell is estimated using the *APES* method, this contribution is subtracted.
One obtain at iteration number p for the range cell r:

$$
\begin{aligned}
\hat{\tilde{\mathbf{Y}}}_t^{(r;p)} &= \hat{\tilde{\mathbf{Y}}}_t^{(r;p-1)} - \hat{\tilde{\mathbf{Y}}}_c^{(r;p)} \\
&= \hat{\tilde{\mathbf{Y}}}_t^{(r;p-1)} - \hat{\alpha}^{(r;p)}\mathbf{s}_s(\theta_r)\left(\mathbf{x}(-\tau_r) \circ \mathbf{s}_d(\tilde{\nu}_{d_{r;p}})\right)^T
\end{aligned} \tag{21}
$$

with $\hat{\tilde{\mathbf{Y}}}_t^{(1;1)} = \tilde{\mathbf{Y}}$ and $\hat{\alpha}^{(r;p)} = \max_p \hat{\alpha}_{r;p}$.

IV. Application to Real Data

This section presents the results obtained applying an iterative rejection thanks to the *APES* method to real ground clutter where a target has been injected. Table I provides the configuration parameters of the measured ground clutter created by the Eiffel Tower $DVB-T$ emitter.

TABLE I
Configuration Parameters

<table>
<tr><th colspan="8">Acquisition parameters</th></tr>
<tr><td>$\tilde{N}_d$</td><td>74</td><td>N_s</td><td>4</td><td>S</td><td>2^{13}</td><td>T_{ci}</td><td>$66ms$</td></tr>
<tr><th colspan="8">Emitter</th></tr>
<tr><td colspan="2">$EIRP$</td><td colspan="2">$20kW$</td><td colspan="2">Central frequency</td><td colspan="2">$562MHz$</td></tr>
<tr><th colspan="8">Target</th></tr>
<tr><td colspan="2">Signal to clutter ratio</td><td colspan="2">$-40dB$</td><td colspan="2">Direction of arrival (θ)</td><td colspan="2">$22°$</td></tr>
<tr><td colspan="2">f_d</td><td colspan="2">$-30Hz$</td><td colspan="2">Range cell (τf_s)</td><td colspan="2">50</td></tr>
</table>

Figure 1 (a) presents a range-Doppler diagram ($\underset{\theta}{max}\,\alpha(\tau,\theta,f_d)$) before rejection. This position is represented by a black cross. The effect of iterative clutter rejection is presented on figure 1 (b). The area of rejection has been chosen between range cell number 20 and range cell number 80. Even if data have been collected from a ground clutter the hypothesis of internal clutter motion has been made. The rejection was applied between $-5Hz$ and $5Hz$ and all over angles between $-90°$ and $90°$. Figure 2 (a) focuses on the range cell 50 where the target has been injected. One can see on this figure that if the target is hidden in a sidelobe of the clutter before rejection, it appears in figure 2 (b) after clutter rejection.

V. Conclusion

We have shown in this paper how efficient the *APES* method could be in the frame of the rejection of ground clutter for a bistatic passive radar.

Acknowledgment

The authors would like to thank François Delaveau and François Pipon (Thales-communications, EDS/SPM/SBP, Colombes, France) for providing raw data.

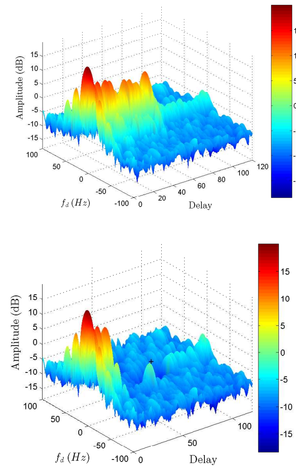

Fig. 1. $\underset{\theta}{max}\,\alpha(\tau,\theta,f_d)$ before (a) and after (b) rejection

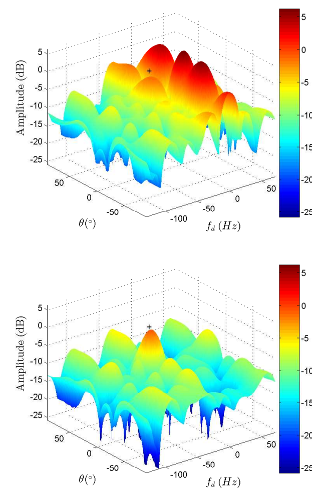

Fig. 2. $\alpha(\theta,f_d)$ in range cell 50 before (a) and after (b) rejection

References

[1] H. Zheng, F. Li, J. Luo, and J. Lu, "Bistatic radar experiment based on FM broadcast transmitter," in *Proc. IEEE Radar Conference, Toulouse, France*, Oct. 19-21 2004.

[2] J. Horner, K. Kubik, B. Mojarrabi, I. D. Longstaff, E. Donskoi, and M. Cherniakov, "Passive bistatic radar sensing with LEOS based transmitters," in *Proc. IGARSS'02, Toronto, Canada*, Jun. 24-28 2002, pp. 438–440.

[3] R. Saini, M. Cherniakov, and V. Lenive, "Direct path interference suppression in bistatic system: DTV based radar," in *Proc. of the International Radar Conference 2003*, Sep. 2003, pp. 309–314.

[4] M. Kubica, V. Kubica, X. Neyt, J. Raout, S. Roques, and M. Acheroy, "Optimum target detection using emitters of opportunity," in *Proc. IEEE Radar Conference, Verona, NY*, Apr. 24-27 2006, pp. 417–424.

[5] H. D. Griffiths and C. J. Baker, "Measurement and analysis of ambiguity functions of passive radar transmissions," in *Proc. IEEE Radar Conference, Arlington, VA*, May 9-12 2005, pp. 321–325.

[6] R. Klemm, *Principles of space-time adaptive processing*. UK: The Institution of Electrical Engineers (IEE), 2002.

[7] J. R. Guerci, *Space-Time Adaptive Processing for Radar*. Norwood, MA: Artech House, 2003.

[8] J. Raout, X.Neyt, and P. Rischette, "Bistatic STAP using illuminators of opportunity," in *Proc. IET Conference on Radar Systems, Edinburgh, Scotland*, Oct. 15-18 2007.

[9] H. Wang and L. Cai, "On adaptive spatial-temporal processing for airborne surveillance radar systems," *IEEE Transactions on the Aerospace and Electronic Systems*, pp. 660–670, Jul. 1994.

[10] M. C. Wicks, M. Rangaswamy, R. Adve, and T. B. Hale, "Space-time adaptive processing : A knowledge-based perspective for airborne radar," *IEEE Signal Processing Magazine*, pp. 51–65, Jan. 2006.

[11] J. Raout and J. P. Préaux, "Multi-target detection using noise-like signals," in *Proc. IEEE Radar Conference, Rome, Italy*, May 26 - 30 2008.

[12] J. Raout, "Space-time adaptive processing for noise-radar," in *Proc. IEEE Radar Conference, Rome, Italy*, May 26 - 30 2008.

[13] J. Li and P. Stoica, "An adaptive filtering approach to spectral estimation and sar imaging," *IEEE Trans. Signal Processing*, vol. 44, no. 2, pp. 1469–1484, Jun. 1996.

[14] H. L. P. Stoica and J. Li, "A new derivation of the APES filter," *IEEE Signal Processing Letters*, vol. 6, pp. 205–206, Aug. 1999.

[15] ——, "Amplitude estimation of sinusoidal signals: survey, new results and an application," *IEEE Trans. Signal Processing*, vol. 48, pp. 338–352, Feb. 2000.

[16] S. Stein, "Algorithms for ambiguity function processing," *IEEE Transactions on Acoustics, Speech and Signal Processing*, vol. 29, no. 3, pp. 588–599, Jun. 1981.